

Flavor Oscillation Modes In Dense Neutrino Media

Huaiyu Duan*

Department of Physics & Astronomy, University of New Mexico, Albuquerque, NM 87131, USA

(Dated: September 29, 2018)

We study two-flavor neutrino oscillations in homogeneous neutrino gases in which neutrinos and anti-neutrinos are in nearly pure weak interaction states initially. We find that the monopole and dipole oscillation modes can trigger flavor instabilities in the opposite neutrino mass hierarchies in a nearly isotropic neutrino gas. For a class of simple neutrino systems we are able to identify the normal modes of neutrino oscillations in the linear regime. Our results provide new insights into the recently discovered multi-azimuthal angle (MAA) instability of neutrino oscillations in supernovae.

PACS numbers: 14.60.Pq, 97.60.Bw

I. INTRODUCTION

The neutrino oscillation phenomenon provides the first piece of solid evidence of the physics beyond the standard model of particle physics (see, e.g. [1, 2] for reviews). Although neutrino oscillations in vacuum and matter are generally well understood, flavor oscillations in dense neutrino media, especially in a core-collapse supernova, are still being intensely investigated, and new phenomena are continuously being discovered, mostly through numerical simulations (e.g. [3–12]; see [13] for a recent but incomplete review). The complexity of the flavor oscillations in a dense neutrino medium lies in the nonlinear, neutrino-neutrino scattering potential which can engender collective neutrino flavor transformation.

To make the problem of collective neutrino oscillations more tractable, certain assumptions were universally adopted. For example, it was assumed that both the number fluxes (or, in terms of transport theory, the 0th angular moment of the distribution function) and flavor content of neutrinos were homogeneous and isotropic in the early Universe (e.g. [14–16]). For core-collapse supernovae it was assumed that both the number fluxes and flavor content of neutrinos were spherically symmetric about the center of the neutron star as well as axially symmetric about any radial direction from the neutron star [17].

In an early study [18] it was shown that angle-dependent flavor transformation can occur in a homogeneous, symmetric, bipolar neutrino gas in which neutrinos and anti-neutrinos have equal densities. It turns out that this phenomenon is much more common than previously expected. It was recently pointed out [19] that, even if the flavor content of supernova neutrinos is (approximately) axially symmetric on the surface of the neutron star, it will no longer be so after the so-called multi-azimuthal angle (MAA) instability of neutrino oscillations has fully developed. This claim seems to be supported by the linear stability analysis [19] and some direct numerical simulations [20, 21]. This finding calls

into question almost all the previous calculations in literature because the existing calculations on collective neutrino oscillations in supernovae, including those in [19–21], assume the flavor content of supernova neutrinos to be spherically symmetric about the neutron star, which is not true once the axial symmetry is broken.

The stability analysis of the linearized equations of motion (e.g. [22–24]) seems straightforward by itself. However, the mathematical criteria for neutrino flavor instabilities that are derived from this method are not necessarily physically transparent or intuitive [25]. To provide some insight for the arise of the MAA instability a simplistic two-beam model was proposed [25]. It was shown that in this model two collective oscillation modes, known as the symmetric and anti-symmetric modes, exist, and they behave like pendulums when the other mode is absent.

In this paper we focus on homogeneous neutrino gases in which angle-dependent neutrino flavor transformation can be studied in a self-consistent way. In Section II we revisit the single-energy, symmetric bipolar systems which were previously studied in literature. We identify the normal modes of these systems in the linear regime. We show that the monopole and dipole modes are unstable in the opposite neutrino mass hierarchies, and that all other multipole modes are stable in the linear regime. In Section III we generalize our study to other homogeneous and isotropic neutrino gases. We also discuss how to use our results to gain new insights into the newly discovered MAA instability of neutrino oscillations in supernovae. In Section IV we give our conclusions.

II. NORMAL OSCILLATION MODES IN MONOCHROMATIC, SYMMETRIC, BIPOLAR NEUTRINO GASES

A. Equations of Motion

For two-flavor neutrino oscillations the flavor content of a neutrino or anti-neutrino can be described by its “flavor isospin” [26]. (See Appendix A for a more detailed discussion of the neutrino flavor isospin.) The flavor isospin of a neutrino can be defined as $\mathbf{s} = \psi^\dagger(\boldsymbol{\sigma}/2)\psi$,

* duan@unm.edu

and that of an anti-neutrino can be defined as $\mathbf{s} = (\sigma_2\psi)^\dagger(\boldsymbol{\sigma}/2)(\sigma_2\psi)$, where ψ is the flavor wavefunction of the neutrino or anti-neutrino, and σ_i ($i = 1, 2, 3$) are the standard Pauli matrices. The flavor isospins of a neutrino and an anti-neutrino of the same energy E are distinguished by their oscillation frequencies $\omega = \pm\Delta m^2/2E$, where the plus and minus signs apply to the neutrino and the anti-neutrino, respectively, and Δm^2 is the neutrino mass-squared difference.

The flavor isospin of a neutrino or an anti-neutrino obeys an equation of motion (EoM) which is similar to that of a magnetic dipole coupled to both the external magnetic field and other dipoles. For a homogeneous neutrino gas one has

$$\begin{aligned} \frac{d}{dt}\mathbf{s}_{\omega,\hat{v}} &= -2\sqrt{2}G_F\mathbf{s}_{\omega,\hat{v}} \times \sum_{\omega',\hat{v}'}(1-\hat{v}\cdot\hat{v}')n_{\omega',\hat{v}'}\mathbf{s}_{\omega',\hat{v}'} \\ &\quad + \mathbf{s}_{\omega,\hat{v}} \times \boldsymbol{\omega}\mathbf{H}_0, \end{aligned} \quad (1)$$

where $\mathbf{s}_{\omega,\hat{v}}$ is the flavor isospin for the neutrino or anti-neutrino with oscillation frequency ω and velocity \hat{v} , G_F is the Fermi coupling constant, and $n_{\omega,\hat{v}}$ is the number density of the corresponding neutrino. For vacuum oscillations \mathbf{H}_0 is a unit vector tilted away from the unit basis vector \mathbf{e}_3 in flavor space by angle 2θ , where θ is the vacuum mixing angle. When a large matter density is present, one can take into account the matter effect by setting $\mathbf{H}_0 \approx \mathbf{e}_3$ and $\theta \ll 1$ [26, 27]. Here we assume that the latter case is true.

Note that the coupling coefficient between two neutrinos of velocities \hat{v} and \hat{v}' is proportional to $1-\hat{v}\cdot\hat{v}'$, which is because of the current-current nature of (low-energy) weak interaction.

Throughout this paper we use the convention that $\hbar = c = 1$, and we assume neutrinos to be relativistic, i.e. $|\hat{v}| = 1$.

In this section we focus on single-energy, symmetric, bipolar systems which were the first systems studied for collective neutrino oscillations [14, 15, 18, 26–29]. We consider a homogeneous neutrino gas which consists of neutrinos and anti-neutrinos of the same energy E_0 . We assume that the neutrino and anti-neutrino of the same velocity \hat{v} have equal number fluxes (i.e. $n_{\omega_0,\hat{v}} = n_{-\omega_0,\hat{v}}$, and thus “symmetric”) and opposite flavor isospins ($\mathbf{s}_{\omega_0,\hat{v}}(0) \approx -\mathbf{s}_{-\omega_0,\hat{v}}(0)$, and thus “bipolar”) at time $t = 0$. In literature it was usually assumed that the neutrino number fluxes were angle independent, i.e. $n_{\omega_0,\hat{v}} = n_{\text{tot}}/4\pi$, where n_{tot} is the total neutrino number density. Here we allow a non-trivial angle distribution

$$f_{\hat{v}} = \frac{n_{\omega_0,\hat{v}}}{n_{\text{tot}}}. \quad (2)$$

For such a system we define

$$\mathbf{d}_{\hat{v}} = \mathbf{s}_{\omega_0,\hat{v}} + \mathbf{s}_{-\omega_0,\hat{v}}, \quad \mathbf{g}_{\hat{v}} = \mathbf{s}_{\omega_0,\hat{v}} - \mathbf{s}_{-\omega_0,\hat{v}}. \quad (3)$$

From Eq. (1) it is easy to show that $\mathbf{d}_{\hat{v}}$ and $\mathbf{g}_{\hat{v}}$ obey EoM

$$\dot{\mathbf{d}}_{\hat{v}} = \eta\mathbf{g}_{\hat{v}} \times \mathbf{H}_0 - \mu\mathbf{d}_{\hat{v}} \times \int (1-\hat{v}\cdot\hat{v}')f_{\hat{v}'}\mathbf{d}_{\hat{v}'} d\Omega_{\hat{v}'}, \quad (4a)$$

$$\dot{\mathbf{g}}_{\hat{v}} = \eta\mathbf{d}_{\hat{v}} \times \mathbf{H}_0 - \mu\mathbf{g}_{\hat{v}} \times \int (1-\hat{v}\cdot\hat{v}')f_{\hat{v}'}\mathbf{d}_{\hat{v}'} d\Omega_{\hat{v}'}. \quad (4b)$$

In the above equations, the dot (“.”) symbol denotes the differentiation with respect to dimensionless time $\tau = |\omega_0|t$, η is the signature of the neutrino mass hierarchy and $\eta = +1$ for the normal neutrino mass hierarchy (NH, $\Delta m^2 > 0$) and -1 for the inverted neutrino mass hierarchy (IH, $\Delta m^2 < 0$), $\mu = 2\sqrt{2}G_F|\omega_0|^{-1}n_{\text{tot}}$ is a dimensionless measure of the interaction strength between flavor isospins (as well as a measure of the neutrino density)¹, and $d\Omega_{\hat{v}'}$ is the differential solid angle with respect to direction \hat{v}' .

We assume that at $\tau = 0$, all the neutrinos and anti-neutrinos are almost purely electron-flavored, i.e. $\mathbf{s}_{\omega_0,\hat{v}}(0) \approx -\mathbf{s}_{-\omega_0,\hat{v}} \approx \mathbf{e}_3/2$. To study the development of collective oscillation modes we shall focus on the linear regime in which

$$|\mathbf{q}_{\hat{v}} \equiv \mathbf{g}_{\hat{v}} - \mathbf{e}_3| \ll 1. \quad (5)$$

In this regime Eq. (4) simplifies as

$$\dot{\mathbf{d}}_{\hat{v}} \approx \eta\mathbf{q}_{\hat{v}} \times \mathbf{H}_0, \quad (6a)$$

$$\dot{\mathbf{q}}_{\hat{v}} \approx \left[\eta\mathbf{d}_{\hat{v}} + \mu \int (1-\hat{v}\cdot\hat{v}')f_{\hat{v}'}\mathbf{d}_{\hat{v}'} d\Omega_{\hat{v}'} \right] \times \mathbf{H}_0, \quad (6b)$$

where we have ignored all the terms of order $\mathcal{O}(|\mathbf{q}_{\hat{v}}|^2)$ or higher.

B. Two Colliding Neutrino Beams

A simple but inspiring example of bipolar system was discussed in [25] which consists of only two neutrino beams with angle distribution

$$f_{\hat{v}} = \frac{1}{2} [\delta(\varphi) + \delta(\varphi - \pi)] \delta(\cos\vartheta), \quad (7)$$

where ϑ and φ are the polar (or zenith) and azimuthal angles of \hat{v} , respectively².

¹ The dimensionless interaction strength μ is always positive for the examples presented in this paper. In general μ can be positive or negative depending on whether the number density of ν_e is larger or smaller than that of the other neutrino flavor. The systems with $\mu < 0$ in certain neutrino mass hierarchy behave like those with $\mu > 0$ but in the opposite mass hierarchy. This can be seen, e.g. by comparing the EoM of the plus and minus modes in Eq. (9).

² The discussions here also apply to the system where two beams do not collide head to head if one makes the replacement $\mu \rightarrow \tilde{\mu} = [1 - \cos(\varphi_1 - \varphi_2)]\mu/2$, where $\varphi_{1(2)}$ is the azimuthal angle of the corresponding beam.

For the two-beam system we define

$$\tilde{\mathbf{d}}_{\pm} = \frac{\mathbf{d}_1 \pm \mathbf{d}_2}{2}, \quad \tilde{\mathbf{q}}_{\pm} = \frac{\mathbf{q}_1 \pm \mathbf{q}_2}{2}, \quad (8)$$

where subscripts 1 and 2 refer to the beams with $\varphi = 0$ and π , respectively. From Eq. (6) we obtain

$$\dot{\tilde{\mathbf{d}}}_+ \approx \eta \tilde{\mathbf{q}}_+ \times \mathbf{H}_0, \quad \dot{\tilde{\mathbf{q}}}_+ \approx (\eta + \mu) \tilde{\mathbf{d}}_+ \times \mathbf{H}_0, \quad (9a)$$

$$\dot{\tilde{\mathbf{d}}}_- \approx \eta \tilde{\mathbf{q}}_- \times \mathbf{H}_0, \quad \dot{\tilde{\mathbf{q}}}_- \approx (\eta - \mu) \tilde{\mathbf{d}}_- \times \mathbf{H}_0. \quad (9b)$$

In other words, the plus and minus modes are independent of each other in the linear regime.

We note that in the linear regime \mathbf{d} 's and \mathbf{q} 's are perpendicular to \mathbf{H}_0 . Therefore,

$$\ddot{\tilde{q}}_+ \approx -\eta(\eta + \mu)\tilde{q}_+, \quad (10)$$

where \tilde{q}_+ is the amplitude of $\tilde{\mathbf{q}}_+$. In the NH case ($\eta = +1$)

$$\tilde{q}_+(\tau) \propto \cos(\gamma\tau), \quad (11)$$

where $\gamma = \sqrt{1 + \eta\mu}$, and the plus mode is always stable. In the IH case ($\eta = -1$), however,

$$\tilde{q}_+(\tau) \propto \begin{cases} e^{\kappa\tau} & \text{if } \mu > 1, \\ \cos(\gamma\tau) & \text{if } \mu < 1, \end{cases} \quad (12)$$

where $\kappa = \sqrt{\mu - 1}$. Therefore, the plus mode is unstable only in the IH case and when $\mu > 1$, and it is stable otherwise.

For the minus mode we note that $(-\tilde{\mathbf{d}}_-, \tilde{\mathbf{q}}_-)$ follow the same EoM of $(\tilde{\mathbf{d}}_+, \tilde{\mathbf{q}}_+)$ but with $\eta \rightarrow -\eta$. Therefore, the minus mode is unstable only in the NH case and when $\mu > 1$.

In Fig. 1 we show the development of the plus and minus modes in the linear regime for a two-beam system with $\mu = 10$. The numerical calculations are in good agreement with the analytic expectations for these modes.

C. An Axial Ring of Neutrino Beams

As another example we consider an axially symmetric ring of neutrino beams with angle distribution

$$f_{\hat{v}} = \frac{1}{2\pi} \delta(\cos \vartheta). \quad (13)$$

For this system we define

$$\tilde{\mathbf{d}}_m = \int_0^{2\pi} \Phi_m^*(\varphi) \mathbf{d}_\varphi d\varphi, \quad (14a)$$

$$\tilde{\mathbf{q}}_m = \int_0^{2\pi} \Phi_m^*(\varphi) \mathbf{q}_\varphi d\varphi, \quad (14b)$$

where $\Phi_m(\varphi) = e^{im\varphi}/\sqrt{2\pi}$ ($m = 0, \pm 1, \pm 2, \dots$) form a complete, orthonormal basis for functions of φ defined on $[0, 2\pi)$.

Because

$$1 - \cos(\varphi - \varphi') = 2\pi \left[\Phi_0(\varphi) \Phi_0^*(\varphi') - \frac{1}{2} \sum_{m=\pm 1} \Phi_m(\varphi) \Phi_m^*(\varphi') \right], \quad (15)$$

the EoM of the modes with different m values are decoupled in the linear regime:

$$\dot{\tilde{\mathbf{d}}}_m \approx \eta \tilde{\mathbf{q}}_m \times \mathbf{H}_0, \quad \dot{\tilde{\mathbf{q}}}_m \approx (\eta + \tilde{\mu}_m) \tilde{\mathbf{d}}_m \times \mathbf{H}_0, \quad (16)$$

where the effective coupling coefficient

$$\tilde{\mu}_m = \begin{cases} \mu & \text{if } m = 0, \\ -\mu/2 & \text{if } m = \pm 1, \\ 0 & \text{otherwise.} \end{cases} \quad (17)$$

We note that the oscillations of the $|m| > 1$ modes do not depend on neutrino densities, and they are always stable. We also note that the angle-independent mode (with $m = 0$) behaves like the plus mode in the two-beam system, and the $m = \pm 1$ modes behave like the minus mode but with the effective neutrino number density reduced by a factor of 1/2.

These results again agree with our numerical calculations (see Fig. 1).

D. Isotropic Neutrino Fluxes

As the last example we look at the bipolar system with isotropic neutrino number fluxes with

$$f_{\hat{v}} = \frac{1}{4\pi}. \quad (18)$$

In literature it was usually assumed that the flavor content of the neutrino fluxes was also isotropic. (In [18] it was assumed that the flavor content of neutrinos was axially symmetric.) We do not make such assumptions here. For the isotropic-flux system we define

$$\tilde{\mathbf{d}}_{l,m} = \int Y_{l,m}^*(\hat{v}) \mathbf{d}_{\hat{v}} d\Omega_{\hat{v}}, \quad (19a)$$

$$\tilde{\mathbf{q}}_{l,m} = \int Y_{l,m}^*(\hat{v}) \mathbf{q}_{\hat{v}} d\Omega_{\hat{v}}, \quad (19b)$$

where $Y_{l,m}$ are the spherical harmonics. Because

$$1 - \hat{v} \cdot \hat{v}' = 4\pi \left[Y_{0,0}(\hat{v}) Y_{0,0}^*(\hat{v}') - \frac{1}{3} \sum_{m=0,\pm 1} Y_{1,m}(\hat{v}) Y_{1,m}^*(\hat{v}') \right], \quad (20)$$

the EoM of the modes with different (l, m) values are decoupled in the linear regime:

$$\dot{\tilde{\mathbf{d}}}_{l,m} \approx \eta \tilde{\mathbf{q}}_{l,m} \times \mathbf{H}_0, \quad \dot{\tilde{\mathbf{q}}}_{l,m} \approx (\eta + \tilde{\mu}_l) \tilde{\mathbf{d}}_{l,m} \times \mathbf{H}_0, \quad (21)$$

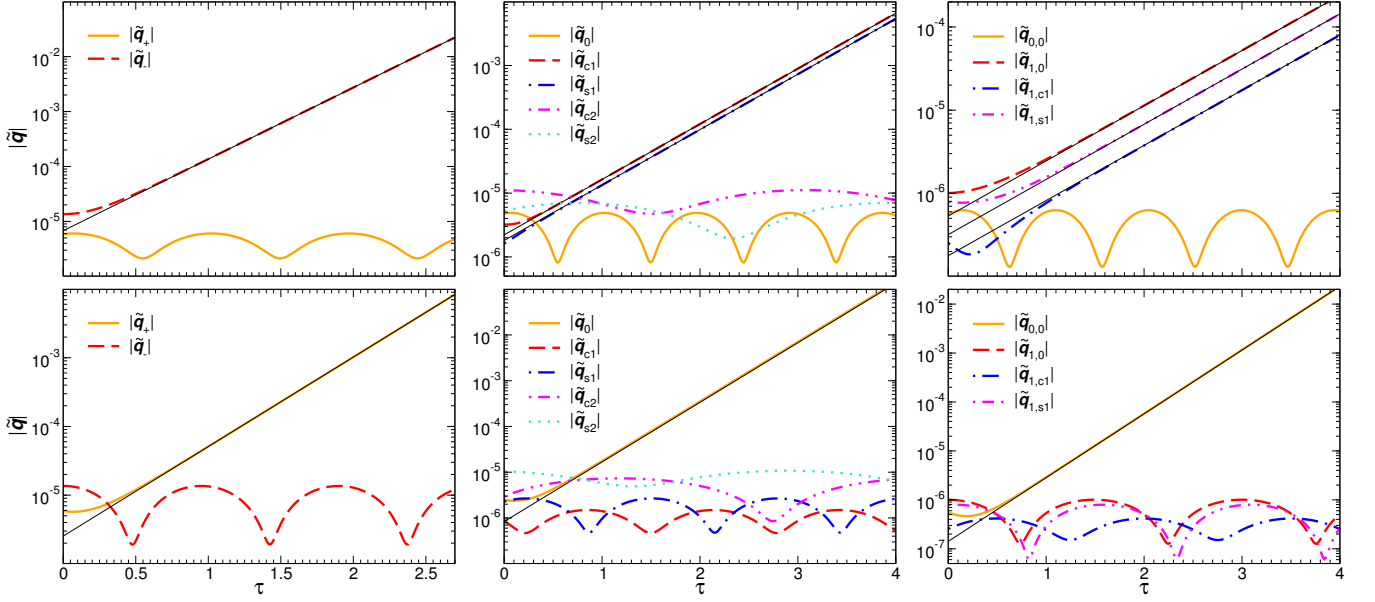


FIG. 1. (Color online) Normal oscillation modes of monochromatic, symmetric, bipolar systems in the linear regime for the normal (upper panels) and inverted (lower panels) neutrino mass hierarchies, respectively. The thick lines (with legends) are the results obtained by solving the equation of motion, i.e. Eq. (1), numerically, and the solid thin lines have the exponential growth rates $\kappa = \sqrt{\mu/2 - 1}$ (the middle top panel), $\sqrt{\mu/3 - 1}$ (the right top panel) and $\sqrt{\mu - 1}$ (the rest of the panels) with $\mu = 10$. For numerical calculations, small random perturbations are seeded at $\tau = 0$ so that $\mathbf{q}_{\hat{v}}(0)$ are not identical for different \hat{v} 's. Left panels: The magnitudes of $\tilde{\mathbf{q}}_{\pm}$ in the two-beam system. Middle panels: The magnitudes of $\tilde{\mathbf{q}}_0$, $\tilde{\mathbf{q}}_{cm} = (\tilde{\mathbf{q}}_m + \tilde{\mathbf{q}}_{-m})/2$ and $\tilde{\mathbf{q}}_{sm} = (\tilde{\mathbf{q}}_m - \tilde{\mathbf{q}}_{-m})/2i$ in the axial-ring system. Right panels: The magnitudes of $\tilde{\mathbf{q}}_{l,0}$, $\tilde{\mathbf{q}}_{l,cm} = (\tilde{\mathbf{q}}_{l,m} + \tilde{\mathbf{q}}_{l,-m})/2$ and $\tilde{\mathbf{q}}_{l,sm} = (\tilde{\mathbf{q}}_{l,m} - \tilde{\mathbf{q}}_{l,-m})/2i$ in the isotropic-flux system.

where the effective coupling coefficient

$$\tilde{\mu}_l = \begin{cases} \mu & \text{if } l = 0, \\ -\mu/3 & \text{if } l = 1, \\ 0 & \text{otherwise.} \end{cases} \quad (22)$$

We note that the $l > 1$ modes in the isotropic-flux system are like the $|m| > 1$ modes in the axial-ring system, and they are always stable. We also note that the monopole mode ($l = 0$) behaves like the plus mode in the two-beam system, and that the dipole modes ($l = 1$) behave like the minus mode but with the effective neutrino number density reduced by $2/3$.

These results indeed agree with our numerical calculations (see Fig. 1).

III. EXTENSIONS AND DISCUSSION

The techniques discussed in Section II can be applied to more general systems. A simple but useful generalization is the monochromatic, homogeneous, isotropic (in terms of neutrino number fluxes), non-symmetric bipolar gas. In a non-symmetric system the number densities of the neutrino and anti-neutrino are not the same but are related by

$$\bar{n}_{\text{tot}} = \alpha n_{\text{tot}}, \quad (23)$$

where \bar{n}_{tot} is the total number density of the anti-neutrino. Again we assume that $\mathbf{s}_{\omega_0, \hat{v}} \approx \mathbf{s}_{-\omega_0, \hat{v}} \approx \mathbf{e}_3/2$ at $\tau = 0$. For such a system we define

$$\mathbf{d}_{\hat{v}} = \mathbf{s}_{\omega_0, \hat{v}} + \alpha \mathbf{s}_{-\omega_0, \hat{v}} - \frac{(1 - \alpha)}{2} \mathbf{e}_3, \quad (24a)$$

$$\mathbf{q}_{\hat{v}} = \mathbf{s}_{\omega_0, \hat{v}} - \alpha \mathbf{s}_{-\omega_0, \hat{v}} - \frac{(1 + \alpha)}{2} \mathbf{e}_3. \quad (24b)$$

In the linear regime where $|\mathbf{q}_{\hat{v}}| \ll 1$ we obtain

$$\begin{aligned} \dot{\mathbf{d}}_{\hat{v}} \approx & \left[\eta \mathbf{q}_{\hat{v}} + (1 - \alpha) \frac{\mu}{2} \int (1 - \hat{v} \cdot \hat{v}') f_{\hat{v}'} \mathbf{d}_{\hat{v}'} d\Omega_{\hat{v}'} \right] \times \mathbf{H}_0 \\ & - (1 - \alpha) \frac{\mu}{2} \mathbf{d}_{\hat{v}} \times \mathbf{H}_0, \end{aligned} \quad (25a)$$

$$\begin{aligned} \dot{\mathbf{q}}_{\hat{v}} \approx & \left[\eta \mathbf{d}_{\hat{v}} + (1 + \alpha) \frac{\mu}{2} \int (1 - \hat{v} \cdot \hat{v}') f_{\hat{v}'} \mathbf{d}_{\hat{v}'} d\Omega_{\hat{v}'} \right] \times \mathbf{H}_0 \\ & - (1 - \alpha) \frac{\mu}{2} \mathbf{q}_{\hat{v}} \times \mathbf{H}_0. \end{aligned} \quad (25b)$$

In the reference frame which rotates about \mathbf{H}_0 by frequency $(1 - \alpha)\mu/2$ we obtain

$$\dot{\tilde{\mathbf{d}}}_{l,m} \approx \left[\eta \tilde{\mathbf{q}}_{l,m} + (1 - \alpha) \frac{\tilde{\mu}_l}{2} \tilde{\mathbf{d}}_{l,m} \right] \times \mathbf{H}_0, \quad (26a)$$

$$\dot{\tilde{\mathbf{q}}}_{l,m} \approx \left[\eta + (1 + \alpha) \frac{\tilde{\mu}_l}{2} \right] \tilde{\mathbf{d}}_{l,m} \times \mathbf{H}_0. \quad (26b)$$

The EoM of \mathbf{d} 's and \mathbf{q} 's again decouple in the spherical basis.

We note that the $l > 1$ modes oscillate with frequencies ω in the co-rotating frame and that they are always stable. The monopole mode (with $l = 0$ and $\tilde{\mu}_0 = \mu$) has been well studied in literature [22, 26, 27, 29]. This mode is unstable only in the IH case and when

$$\frac{4}{(1 + \sqrt{\alpha})^2} < \mu < \frac{4}{(1 - \sqrt{\alpha})^2}. \quad (27)$$

For the dipole modes (with $l = 1$ and $\tilde{\mu}_1 = -\mu/3$) we note that $(-\mathbf{d}_{1,m}, \mathbf{q}_{1,m})$ obey the same EoM of $(\mathbf{d}_{0,0}, \mathbf{q}_{0,0})$ except with replacements

$$\eta \rightarrow -\eta, \quad \mu \rightarrow \frac{\alpha\mu}{3}, \quad \alpha \rightarrow \alpha^{-1}. \quad (28)$$

This implies that the dipole modes are unstable only in the NH case and when

$$\frac{12}{(1 + \sqrt{\alpha})^2} < \mu < \frac{12}{(1 - \sqrt{\alpha})^2}. \quad (29)$$

One can further generalize these techniques to homogeneous and isotropic neutrino gases with continuous energy spectra. In such systems the oscillation modes with different (l, m) are not coupled in the linear regime. The monopole modes with different ω 's are coupled, and these modes can engender the angle-independent collective flavor transformation which was studied in the literature for neutrino oscillations in the early Universe and that for the single-angle approximation of supernova neutrinos. The dipole modes with different ω 's are also coupled. The results of the monopole modes can be applied to the dipole modes with appropriate replacements similar to Eq. (28).

We note that, however, the multipole modes are no longer decoupled once the unstable monopole or dipole modes grow out of the linear regime. The convolution of the multipole modes can but not always result in kinematic decoherence [18, 30]. In any case, it is not always justified to assume that the flavor content of neutrino fluxes will remain isotropic even if both the number fluxes and the flavor content of a homogeneous neutrino gas are (approximately) isotropic initially.

The geometric nature of the supernova environment is much more complicated than that of a homogeneous neutrino gas. A generalization to the ‘‘neutrino bulb model’’ [17] was studied in [19–21]. Like in the original bulb model, both the number fluxes and the flavor content of neutrinos in the generalized bulb model are spherically symmetric about the center of the neutron star at all radii, and they are also axially symmetric about any radial direction on the surface of the neutron star. In the generalized bulb model, however, the flavor content of neutrinos are not assumed to be axially symmetric at all radii.

Because of the initial axial symmetry on the surface of the neutron star, one can apply the techniques discussed for the axial-ring and isotropic-flux models in Section II to the generalized bulb model. It is straightforward to

see that the $|m| > 1$ modes should always be stable in the linear regime. It is also obvious that the newly discovered MAA modes have $m = \pm 1$ and behave like the minus modes in the two-beam systems. The well known bipolar/bimodal mode and the newly discovered multi-zenith-angle (or MZA) mode [19] both have $m = 0$ ³.

As in the axial-ring model, the bipolar and MAA modes in the generalized bulb model are responsible for the flavor instabilities in the opposite neutrino mass hierarchies. This result indeed agrees with what was shown in [19]. In addition, the effective neutrino number densities of the MAA modes is a fraction of that of the bipolar mode. (This fraction can be different from those in the axial-ring and isotropic-flux models because of their different dependence of the neutrino beams and, therefore, the neutrino-neutrino scattering potential, on polar angles.) This implies that the MAA modes can become unstable closer to the neutron star than the bipolar mode does. [One can see this by, e.g. comparing Eq. (29) to (27).] This result also agrees with what was shown in [19].

We emphasize that the generalized bulb model studied in [19–21] is not entirely self-consistent because the MAA modes break the axial symmetry about the radial direction. Even if the bipolar mode is unstable in the linear regime, the azimuthal-angle dependent and independent modes become coupled once the unstable mode(s) grows out of the linear regime, which can also break the axial symmetry. In a supernova neutrino model the spherical symmetry breaks down once the axial symmetry about any radial direction is lost. Therefore, one needs to go beyond the spherical supernova model in studying azimuthal-angle-dependent collective neutrino oscillations even if everything else (the matter density, over all neutrino number fluxes, etc) in the supernova is spherically symmetric.

IV. CONCLUSIONS

We have studied the flavor oscillation modes in homogeneous neutrino gases. We have identified the normal modes of neutrino oscillations in the linear regime for the monochromatic two-beam, axial-ring and isotropic-flux neutrino systems with the symmetric bipolar configuration. We have shown that, because of the current-current nature of (low-energy) weak interaction, only the monopole and dipole modes (or the plus/symmetric and minus/anti-symmetric modes in the case of a two-beam system) could trigger significant flavor transformation in

³ In a private communication with the author G. Raffelt pointed out that, in contrast to the three degenerate dipole modes in a homogeneous, isotropic neutrino gas, the MZA mode and two MAA modes of supernova neutrinos are not degenerate because of the special geometry of the neutrino bulb model.

the opposite neutrino mass hierarchies. All other multipole modes are stable in the linear regime.

We have also discussed how to generalize the results found in the above models to other systems such as non-symmetric bipolar gases and homogeneous, isotropic gases with continuous neutrino energy spectra.

Our study provides new insights into the recent discovery of the MAA flavor instabilities of supernova neutrinos. The bipolar mode and the MZA mode in the generalized neutrino bulb model are the $m = 0$ modes while the MAA modes have $m = \pm 1$. The bipolar mode and the MZA/MAA modes are responsible for flavor instabilities in different neutrino mass hierarchies. The MAA modes can become unstable at a radius smaller than that of the bipolar mode in the opposite neutrino mass hierarchy, which makes them more interesting for supernova nucleosynthesis. However, we also note that, if the azimuthal-angle dependent modes are ever important (whether inside or outside the linear regime), supernova neutrinos cannot be treated self-consistently in a spherical supernova model anymore.

Appendix A: Equations of Motion for Neutrino Oscillations

1. Flavor Density Matrix

For two-flavor neutrino oscillations the flavor density matrix of the neutrino is

$$\rho = \begin{bmatrix} \rho_{ee} & \rho_{ex} \\ \rho_{ex}^* & \rho_{xx} \end{bmatrix}. \quad (\text{A1})$$

The diagonal elements of ρ give the occupation numbers of the neutrino in the e and x flavors, respectively, and the off-diagonal elements contain the information of flavor mixing. The flavor density matrix $\bar{\rho}$ for the anti-neutrino is defined in a similar way. In a homogeneous neutrino gas ρ and $\bar{\rho}$ have no spatial dependence. In absence of collisions, they obey the equations of motion (EoM) [31]

$$i \frac{d}{dt} \rho_{\vec{p}} = [\mathbf{H}_0 + \mathbf{H}_{\text{matt}} + \mathbf{H}_{\nu\nu}(t, \hat{v}), \rho_{\vec{p}}], \quad (\text{A2a})$$

$$i \frac{d}{dt} \bar{\rho}_{\vec{p}} = [\mathbf{H}_0 - \mathbf{H}_{\text{matt}} - \mathbf{H}_{\nu\nu}^*(t, \hat{v}), \bar{\rho}_{\vec{p}}] \quad (\text{A2b})$$

for a homogeneous neutrino gas, where \vec{p} is the momentum of the neutrino or anti-neutrino, $\hat{v} = \vec{p}/E$ is its velocity, and \mathbf{H}_0 , \mathbf{H}_{matt} and $\mathbf{H}_{\nu\nu}$ are the vacuum, matter and neutrino self-coupling (or neutrino-neutrino forward-scattering) parts of the Hamiltonian, respectively.

The vacuum Hamiltonian is

$$\mathbf{H}_0 = \frac{\Delta m^2}{4E} \begin{bmatrix} -\cos 2\theta & \sin 2\theta \\ \sin 2\theta & \cos 2\theta \end{bmatrix}, \quad (\text{A3})$$

where θ is the vacuum mixing angle, and $\Delta m^2 = m_2^2 - m_1^2$ is the mass-squared difference between mass eigenstates $|\nu_1\rangle$ and $|\nu_2\rangle$.

The matter Hamiltonian is

$$\mathbf{H}_{\text{matt}} = \sqrt{2} G_{\text{F}} n_e \begin{bmatrix} 1 & 0 \\ 0 & 0 \end{bmatrix}, \quad (\text{A4})$$

where G_{F} is the Fermi coupling constant, and n_e is the net electron number density. For a homogeneous neutrino gas, a large matter density effectively sets the vacuum mixing angle to a small value [26, 27, 32]. We assume this is the case, and we set $\mathbf{H}_{\text{matt}} = 0$ and $\theta \approx 0$.

The neutrino self-coupling Hamiltonian is [33–35]

$$\mathbf{H}_{\nu\nu}(t, \hat{v}) = \sqrt{2} G_{\text{F}} \sum_{\vec{p}'} (1 - \hat{v} \cdot \hat{v}') [\rho_{\vec{p}'}(t) - \bar{\rho}_{\vec{p}'}^*(t)]. \quad (\text{A5})$$

2. Neutrino Flavor Isospin

To visualize the evolution of flavor density matrices, we use the concept of the neutrino flavor isospin defined in [26]. The flavor density matrix ρ and flavor isospin \mathbf{s} of the same neutrino are related by

$$\rho_{\vec{p}} = \frac{n_{\vec{p}}}{2} + n_{\omega, \hat{v}} \boldsymbol{\sigma} \cdot \mathbf{s}_{\omega, \hat{v}}, \quad (\text{A6a})$$

$$\bar{\rho}_{\vec{p}}^* = \frac{\bar{n}_{\vec{p}}}{2} + n_{-\omega, \hat{v}} \boldsymbol{\sigma} \cdot (-\mathbf{s}_{-\omega, \hat{v}}), \quad (\text{A6b})$$

where

$$n_{\vec{p}} = \rho_{ee, \vec{p}} + \rho_{xx, \vec{p}} \quad \text{and} \quad \bar{n}_{\vec{p}} = \bar{\rho}_{ee, \vec{p}} + \bar{\rho}_{xx, \vec{p}} \quad (\text{A6c})$$

are the number densities of the neutrino and anti-neutrino of momentum \vec{p} , respectively, σ_i ($i = 1, 2, 3$) are the Pauli matrices,

$$\omega = \frac{\Delta m^2}{2E} \quad (\text{A7})$$

is the vacuum oscillation frequency, and $n_{\pm\omega, \hat{v}}$ is the effective density distribution of the neutrino. We use the convention that a bold symbol (e.g. \mathbf{s}) denotes a vector in flavor space, and a symbol with the vector hat (e.g. \hat{p}) denotes a vector in coordinate space.

The flavor density matrix formalism and the flavor isospin formalism are completely equivalent in the two-flavor scheme. In absence of collision neither the trace of a flavor density matrix nor the effective density distribution $n_{\omega, \hat{v}}$ changes over time. Therefore, we ignore the traces of flavor density matrices which have no impact on neutrino oscillations.

Also note that the flavor content of a neutrino is represented by a flavor isospin with $\omega > 0$ ($\omega < 0$) for the normal (inverted) mass hierarchy with $\Delta m^2 > 0$ ($\Delta m^2 < 0$). If the neutrino is in a pure (flavor) quantum state and is represented by flavor wavefunction ψ , then the flavor isospin can be equivalently defined as

$$\mathbf{s} = \psi^\dagger \frac{\boldsymbol{\sigma}}{2} \psi. \quad (\text{A8})$$

Similarly, the flavor content of an anti-neutrino is represented by a flavor isospin with $\omega < 0$ ($\omega > 0$) if $\Delta m^2 > 0$ ($\Delta m^2 < 0$). For an anti-neutrino represented by flavor wavefunction ψ , its flavor isospin is

$$\mathbf{s} = (\sigma_2 \psi)^\dagger \frac{\boldsymbol{\sigma}}{2} (\sigma_2 \psi). \quad (\text{A9})$$

In particular, a pure ν_e is represented by $\mathbf{s} = \mathbf{e}_3/2$, and a pure $\bar{\nu}_e$ is represented by $\mathbf{s} = -\mathbf{e}_3/2$, where \mathbf{e}_i ($i = 1, 2, 3$) are the basis unit vectors in flavor space like \hat{x} , \hat{y} and \hat{z} in coordinate space.

The EoM for the flavor isospin is

$$\begin{aligned} \frac{d}{dt} \mathbf{s}_{\omega, \hat{v}} &= -2\sqrt{2} G_F \mathbf{s}_{\omega, \hat{v}} \times \sum_{\omega', \hat{v}'} (1 - \hat{v} \cdot \hat{v}') n_{\omega', \hat{v}'} \mathbf{s}_{\omega', \hat{v}'} \\ &+ \mathbf{s}_{\omega, \hat{v}} \times \boldsymbol{\omega} \mathbf{H}_0, \end{aligned} \quad (\text{A10})$$

where $\mathbf{H}_0 \approx \mathbf{e}_3$ (because we set vacuum mixing angle $\theta \approx 0$).

One of the main advantages of the concept of flavor isospin is that the neutrino and the anti-neutrino are treated on an equal footing in this formalism.

ACKNOWLEDGMENTS

The author thanks G. Raffelt for reading the draft and providing helpful suggestions. The author also thanks Y.-Z. Qian and S. Shashank for useful discussions. This work was supported in part by DOE grant de-sc0008142 at UNM.

-
- [1] J. Beringer *et al.* (Particle Data Group), Phys.Rev. **D86**, 010001 (2012).
 - [2] A. Strumia and F. Vissani, (2006), hep-ph/0606054.
 - [3] H. Duan, G. M. Fuller, J. Carlson, and Y.-Z. Qian, Phys. Rev. Lett. **97**, 241101 (2006), astro-ph/0608050.
 - [4] H. Duan, G. M. Fuller, J. Carlson, and Y.-Z. Qian, Phys. Rev. Lett. **99**, 241802 (2007), arXiv:0707.0290 [astro-ph].
 - [5] B. Dasgupta, A. Dighe, and A. Mirizzi, Phys. Rev. Lett. **101**, 171801 (2008), arXiv:0802.1481 [hep-ph].
 - [6] H. Duan, G. M. Fuller, J. Carlson, and Y.-Z. Qian, Phys. Rev. Lett. **100**, 021101 (2008), arXiv:0710.1271 [astro-ph].
 - [7] B. Dasgupta, A. Dighe, G. G. Raffelt, and A. Y. Smirnov, Phys. Rev. Lett. **103**, 051105 (2009), arXiv:0904.3542 [hep-ph].
 - [8] J. Gava, J. Kneller, C. Volpe, and G. C. McLaughlin, Phys. Rev. Lett. **103**, 071101 (2009), arXiv:0902.0317 [hep-ph].
 - [9] A. Friedland, Phys. Rev. Lett. **104**, 191102 (2010), arXiv:1001.0996 [hep-ph].
 - [10] H. Duan and A. Friedland, Phys. Rev. Lett. **106**, 091101 (2011), arXiv:1006.2359 [hep-ph].
 - [11] S. Chakraborty, T. Fischer, A. Mirizzi, N. Saviano, and R. Tomas, Phys. Rev. Lett. **107**, 151101 (2011), arXiv:1104.4031 [hep-ph].
 - [12] J. F. Cherry, J. Carlson, A. Friedland, G. M. Fuller, and A. Vlasenko, Phys. Rev. Lett. **108**, 261104 (2012), arXiv:1203.1607 [hep-ph].
 - [13] H. Duan, G. M. Fuller, and Y.-Z. Qian, Ann. Rev. Nucl. Part. Sci. **60**, 569 (2010), arXiv:1001.2799 [hep-ph].
 - [14] V. A. Kostelecký, J. T. Pantaleone, and S. Samuel, Phys. Lett. **B315**, 46 (1993).
 - [15] V. A. Kostelecký and S. Samuel, Phys. Lett. **B318**, 127 (1993).
 - [16] K. N. Abazajian, J. F. Beacom, and N. F. Bell, Phys. Rev. **D66**, 013008 (2002), astro-ph/0203442.
 - [17] H. Duan, G. M. Fuller, J. Carlson, and Y.-Z. Qian, Phys. Rev. **D74**, 105014 (2006), astro-ph/0606616.
 - [18] G. G. Raffelt and G. G. R. Sigl, Phys. Rev. **D75**, 083002 (2007), hep-ph/0701182.
 - [19] G. Raffelt, S. Sarikas, and D. d. S. Seixas, Phys. Rev. Lett. **111**, 091101 (2013), arXiv:1305.7140 [hep-ph].
 - [20] A. Mirizzi, (2013), arXiv:1308.1402 [hep-ph].
 - [21] A. Mirizzi, (2013), arXiv:1308.5255 [hep-ph].
 - [22] A. Banerjee, A. Dighe, and G. Raffelt, Phys.Rev. **D84**, 053013 (2011), arXiv:1107.2308 [hep-ph].
 - [23] S. Sarikas, D. d. S. Seixas, and G. Raffelt, Phys.Rev. **D86**, 125020 (2012), arXiv:1210.4557 [hep-ph].
 - [24] D. Väänänen and C. Volpe, Phys. Rev. **D86**, 065003 (2013), arXiv:1306.6372 [hep-ph].
 - [25] G. Raffelt and D. d. S. Seixas, Phys. Rev., **D88**, 045031 (2013), arXiv:1307.7625 [hep-ph].
 - [26] H. Duan, G. M. Fuller, and Y.-Z. Qian, Phys. Rev. **D74**, 123004 (2006), astro-ph/0511275.
 - [27] S. Hannestad, G. G. Raffelt, G. Sigl, and Y. Y. Y. Wong, Phys. Rev. **D74**, 105010 (2006), astro-ph/0608695.
 - [28] S. Pastor, G. G. Raffelt, and D. V. Semikoz, Phys. Rev. **D65**, 053011 (2002), hep-ph/0109035.
 - [29] H. Duan, G. M. Fuller, J. Carlson, and Y.-Z. Qian, Phys. Rev. **D75**, 125005 (2007), astro-ph/0703776.
 - [30] A. Esteban-Pretel, S. Pastor, R. Tomas, G. G. Raffelt, and G. Sigl, Phys. Rev. **D76**, 125018 (2007), arXiv:0706.2498 [astro-ph].
 - [31] G. Sigl and G. Raffelt, Nucl. Phys. **B406**, 423 (1993).
 - [32] H. Duan, G. M. Fuller, and Y.-Z. Qian, Phys. Rev. **D77**, 085016 (2008), arXiv:0801.1363 [hep-ph].
 - [33] G. M. Fuller, R. W. Mayle, J. R. Wilson, and D. N. Schramm, Astrophys. J. **322**, 795 (1987).
 - [34] D. Nötzold and G. Raffelt, Nucl. Phys. **B307**, 924 (1988).
 - [35] J. T. Pantaleone, Phys. Rev. **D46**, 510 (1992).